Transmission Waiting Time: A Unifying Metric for Outbreak Controllability

Christopher Y. Shin[1,2,3,4], Sang Woo Park[5], Cécile Viboud[4], Pardis C. Sabeti[2, 6, 7, 8, 9], Christophe Fraser[10], and Kaiyuan Sun[4 *]

[1]Harvard College, Harvard University, Cambridge, MA, USA
[2]Broad Institute of MIT and Harvard, Cambridge, MA, USA
[3]Harvard Global Health Institute, Harvard University, Cambridge, MA, USA
[4]Division of International Epidemiology and Population Studies, Fogarty International Center, National Institutes of Health, Bethesda, MD, USA
[5]School of Biological Sciences, Seoul National University, Seoul, South Korea
[6]Howard Hughes Medical Institute, Chevy Chase, MD, USA
[7]Department of Organismic and Evolutionary Biology, Harvard University, Cambridge, MA, USA
[8]Department of Immunology and Infectious Diseases, Harvard T.H. Chan School of Public Health, Harvard University, Boston, MA, USA
[9]Department of Medicine, Division of Infectious Diseases, Massachusetts General Hospital, Boston, MA, USA
[10]Pandemic Sciences Institute, Nuffield Department of Medicine, University of Oxford, Oxford, United Kingdom
[*]Corresponding author: Kaiyuan Sun, kaiyuan.sun@nih.gov

Abstract

Traditional outbreak containment strategies—such as isolating symptomatic individuals and tracing their contacts—often fall short for pathogens with substantial pre-symptomatic or asymptomatic transmission, as exemplified by SARS-CoV-2. This challenge was met by technological advances during the COVID-19 pandemic: widespread, low-cost molecular testing enabled population-scale screening independent of symptoms, while digital tools such as mobile exposure notifications and backward contact tracing improved the speed and precision of response efforts. These advances redefined the landscape of non-pharmaceutical interventions, shifting the focus from symptom-based interventions to proactive, testing-driven identification and isolation of infections.

Here, we introduce a theoretical framework centered on the transmission waiting time—the interval between an individual's infection and their first onward transmission—as a critical benchmark for outbreak control. This framework integrates key pathogen properties, such as the basic reproduction number (R_0) and the generation interval, with operational parameters including the speed and coverage of isolation. We analytically derive the transmission waiting time distribution under a homogeneous mixing assumption and extend the framework to incorporate transmission heterogeneity, demonstrating its utility in establishing temporal thresholds for effective containment.

Applying this framework across a wide range of pathogens reveals substantial variation in controllability, with pathogens that are highly transmissible and/or have shorter generation intervals placing stricter demands on the speed and reach of interventions. Simulation-based analyses further underscore the necessity of optimizing both the timeliness and coverage of isolation efforts.

Taken together, our framework provides clear, biologically grounded metrics for guiding epidemic containment strategies, offering flexible and scalable benchmarks tailored to modern public health response capabilities.

Introduction

A central question in infectious disease control is whether an outbreak can be effectively contained given the transmission characteristics of the causative pathogen and the available intervention strategies [1, 2]. Classical non-pharmaceutical interventions—most notably, the isolation of symptomatic cases and the tracing and quarantining of their contacts—have served as the most common tools for outbreak response. These longstanding measures were pivotal in controlling pathogens such as smallpox, Ebola, and SARS-CoV-1, and were instrumental in the eradication of smallpox when coupled with ring vaccination campaigns [3, 4, 5]. Following the 2003 SARS-CoV-1 epidemic, a seminal study by Fraser et al. introduced a quantitative framework to assess a pathogen's controllability through symptom-based contact-tracing strategies [1]. Their analysis revealed that a pathogen's intrinsic transmissibility—quantified by the basic reproduction number (R_0)—and the extent of pre-symptomatic transmission are key determinants of the effectiveness of these interventions.

The COVID-19 pandemic fundamentally challenged the classical framework for outbreak control, as the extensive pre-symptomatic and asymptomatic transmission of SARS-CoV-2 rendered traditional symptom-based interventions insufficient for effective containment [6, 7, 8, 9, 10, 11]. This challenge was met by technological advances: widespread, low-cost molecular testing enabled population-scale screening to track the virus's cryptic spread, while digital tools like mobile exposure notifications and backward contact tracing enhanced the speed and precision of the response [12, 13, 14]. These tools, acting in synergy with lockdowns that restricted mobility, successfully suppressed community transmission by overcoming the limitations of conventional approaches. These modernized strategies allowed several countries to achieve early containment of pre-Omicron strains, while others adapted mitigation efforts to their unique epidemiological and societal contexts [15, 16, 17, 18, 19].

In light of these developments, we revisit Fraser et al.'s mathematical framework through the lens of a modernized intervention landscape that no longer relies primarily on symptomatic case detection. Specifically, we center our analysis on the concept of the characteristic timescale of outbreak control—a unifying parameter that encapsulates how quickly infections must be identified and isolated to surpess sustained onward transmission. This metric integrates key factors influencing containment success, combining pathogen characteristics (e.g., generation interval and basic reproduction number) with the operational effectiveness of interventions that can act irrespective of symptoms, such as proactive routine testing, targeted tracing, and population-wide measures.

In this study, we introduce a theoretical framework that defines the characteristic timescale of outbreak control, centering on the transmission waiting time distribution—a measure of how quickly onward transmission typically occurs following infection. Using a stylized homogeneous mixing model, we derive an analytical connection between the transmission waiting time and the critical isolation delay distribution required to suppress transmission. We then extend the framework to incorporate partial isolation coverage and individual-level transmission heterogeneity, demonstrating that the core results remain robust under these generalizations. To assess practical relevance, we apply this framework to a diverse set of real-world pathogens, quantifying how intrinsic transmission characteristics constrain the feasibility of containment. Finally, we evaluate the effectiveness of test-trace-isolate (TTI) interventions using branching process simulations, highlighting how operational parameters such as testing sensitivity, routine testing frequency, isolation speed and coverage jointly determine the likelihood of successful outbreak control. Together, these analyses offer a unified and generalizable approach to quantifying the timing requirements for TTI strategies to achieve effective epidemic containment.

The Transmission Waiting Time as the Critical Intervention Timescale for Outbreak Control

The classical infectious disease outbreak controllability framework, formalized by Fraser et al., relies on isolating symptomatic cases and tracing their contacts [1]. However, this paradigm shifted in the post-COVID-19 era where widespread routine asymptomatic testing is possible, allowing infections to be detected regardless of symptoms or links to known cases [7, 9, 6, 8, 10, 20]. For pathogens with significant asymptomatic and pre-symptomatic transmission, the central challenge is no longer limited by the constraints of symptom-based surveillance but is instead reframed around the speed of intervention: how rapidly must infections be isolated, on average, to suppress an epidemic?

We characterize the speed of this individual-based intervention using the isolation delay distribution, $\delta_{\text{iso}}(\tau)$, which is the probability density of time from an individual's infection to their isolation. The objective is to determine the critical intervention timescale, denoted $\delta^*_{\text{iso}}(\tau)$, that must be achieved to bring the effective reproduction number (R_e) below 1.

Achieving containment ($R_e < 1$) intuitively requires isolating most infectious individuals before they have the opportunity to transmit the pathogen. This sets up a race between the public health intervention and pathogen transmission. Accordingly, we define the transmission waiting time, $t_w(\tau)$, as the interval between a primary infection and its first onward transmission. This timescale, intrinsic to the pathogen, represents the fundamental speed barrier that intervention strategies must meet for successful outbreak containment.

In the following sections, we formalize this relationship by deriving the distribution of $t_w(\tau)$. We demonstrate that it provides an asymptotic upper bound on the critical isolation delay, $\delta^*_{\text{iso}}(\tau)$, in a homogeneously mixing population, and show how this temporal bound is shaped by key pathogen characteristics like the basic reproduction number and the generation interval.

Analytical Expression for Transmission Waiting Time Under a Homogeneous Mixing Assumption

To quantify the timing of the earliest secondary transmission event generated by an infected individual, we adopt a survival analysis framework. Specifically, we define the transmission waiting time, $t_w(\tau)$, as the interval between the time of primary infection and the occurrence of the first secondary transmission. This interval is modeled as a "first-hitting-time" problem, governed by a hazard function that captures the time-varying infectiousness of the infected individual [21].

Under the homogeneous mixing assumption, the time-varying transmissibility of an infected individual is fully characterized by the basic reproduction number R_0 and the generation interval distribution $g(\tau)$. The hazard function for secondary transmission at time τ is given by:

$$h(\tau) = R_0 g(\tau) \tag{1}$$

where $g(\tau)$ is the probability density function (PDF) of the generation interval, satisfying the normalization condition:

$$\int_0^\infty g(\tau)\, d\tau = 1 \tag{2}$$

The corresponding survival function, $S(\tau)$—the probability that no secondary transmission has occurred by time τ—is:

$$S(\tau) = \exp\left(-\int_0^\tau h(s)\, ds\right) = \exp\left(-R_0 G(\tau)\right) \tag{3}$$

where $G(\tau) = \int_0^\tau g(s)\,ds$ is the cumulative distribution function (CDF) of the generation interval.

Given the survival function, the cumulative distribution function of the time of the first secondary transmission (i.e. the "first hitting time") is:

$$F(\tau) = 1 - S(\tau) \tag{4}$$

and the corresponding probability density function (PDF) is:

$$f(\tau) = \frac{dF(\tau)}{d\tau} = h(\tau)S(\tau) = R_0\, g(\tau)\, \exp\left(-R_0 G(\tau)\right) \tag{5}$$

Since $S(\infty) = \exp(-R_0)$, it follows that $F(\infty) = 1 - \exp(-R_0) < 1$. This indicates that $f(\tau)$ is a defective density function that does not integrate to one, reflecting the non-zero probability that an infected individual causes no secondary transmissions. Conditioned on the occurrence of at least one secondary transmission, the normalized transmission waiting time distribution is:

$$t_w(\tau) = \frac{f(\tau)}{F(\infty)} = \frac{h(\tau)S(\tau)}{F(\infty)} = \frac{R_0\, g(\tau)\, \exp(-R_0 G(\tau))}{1 - \exp(-R_0)} \tag{6}$$

Here, R_0 determines the average number of secondary transmissions, while the generation interval distribution $g(\tau)$ governs the timing of those events. Together, these parameters shape the transmission waiting time distribution $t_w(\tau)$, which characterizes how fast secondary transmission is expected to occur following a primary infection.

Figure 1 illustrates how variations in R_0 and the generation interval distribution (gamma-distributed) influence the timing of $t_w(\tau)$. For pathogens with the same generation interval distribution, higher values of R_0 result in earlier transmission events, reflected by a leftward shift in $t_w(\tau)$ (panel A). Conversely, for a fixed R_0, shorter mean generation intervals yield earlier and more sharply peaked $t_w(\tau)$ distributions (panel B).

Further, stochastic ordering analysis (Supplementary Materials Section 1) confirms the following relationships for a generalized generation interval distribution $g(\tau)$:

- For a fixed generation interval distribution $g(\tau)$, increasing R_0 shifts $t_w(\tau)$ to earlier times.
- For a fixed R_0, pathogens with stochastically smaller generation interval distributions (i.e., $g(\tau)$ with a shorter mean) exhibit earlier $t_w(\tau)$.

The combined influence of R_0 and $g(\tau)$ defines the characteristic time scale of $t_w(\tau)$. Building on this foundation, the next section explores how $t_w(\tau)$ informs the critical isolation delay distribution $\delta^*_{\text{iso}}(\tau)$, which determines the timing requirements for effective outbreak control.

Transmission Waiting Time Determines the Speed and Coverage of Effective Intervention

To suppress an epidemic with a Test-Trace-Isolate (TTI) strategy, isolation-based interventions must outpace pathogen transmission [22, 23, 24]. We propose the transmission waiting time, $t_w(\tau)$—the time until an infected individual causes any secondary infection—as the key benchmark to determine the required speed and coverage of such interventions.

The success of a TTI strategy depends on its coverage and its speed. Specifically, the intervention coverage, denoted P_{iso}, is the proportion of infected individuals who are successfully isolated.

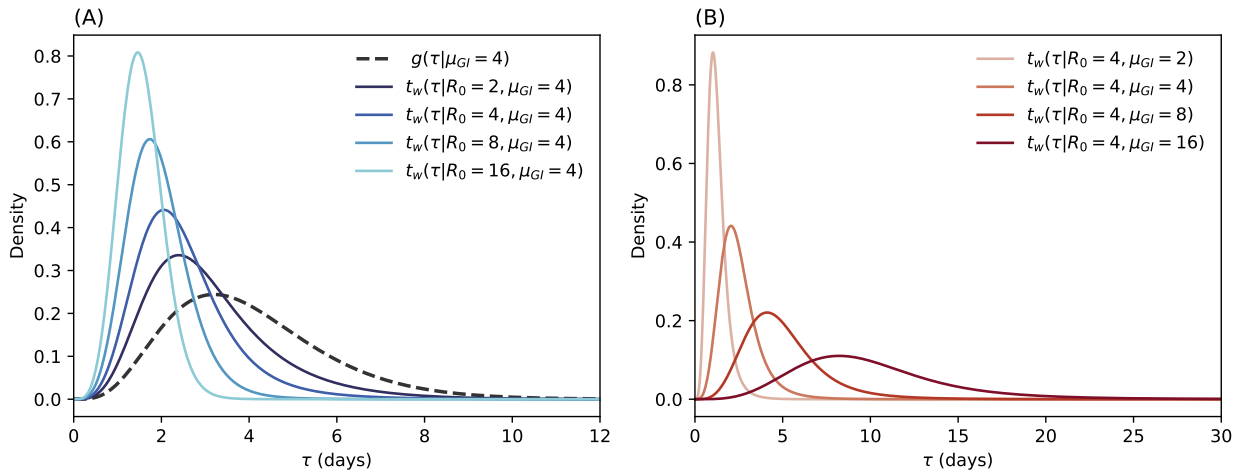

Figure 1: **Transmission waiting time distribution $t_w(\tau)$ under varying generation interval means and reproduction numbers.** (A) Effect of increasing the basic reproduction number R_0 on the transmission waiting time distribution $t_w(\tau)$, given a fixed, gamma-distributed generation interval $g(\tau)$ with mean 4 days and shape parameter $k = 5$. The underlying generation interval distribution $g(\tau)$ is shown as a dashed line. (B) Effect of increasing the mean generation interval μ_{GI} on $t_w(\tau)$, while holding $R_0 = 4$ and $k = 5$ constant. In both panels, higher values of R_0 or shorter μ_{GI} shift $t_w(\tau)$ toward earlier times, indicating a narrower window for intervention.

The corresponding intervention speed among those infections is characterized by the isolation delay distribution, $\delta_{\text{iso}}(\tau)$. Together, these parameters determine the probability that an infected individual remains unisolated at time τ, which is given by the isolation survival function, $S_{\text{iso}}(\tau)$:

$$S_{\text{iso}}(\tau) = 1 - P_{\text{iso}}\Delta_{\text{iso}}(\tau) \tag{7}$$

where $\Delta_{\text{iso}}(\tau) = \int_0^\infty \delta_{iso}(\tau)d\tau$, the cumulative distribution function (CDF) of the isolation delay.

The effective transmission hazard under intervention, $h_e(\tau)$, is the product of the baseline hazard, $h(\tau)$, and the isolation survival function:

$$h_e(\tau) = h(\tau)\, S_{\text{iso}}(\tau) = R_0 g(\tau) S_{\text{iso}}(\tau) \tag{8}$$

Integrating this effective hazard over time yields the effective reproduction number under intervention, R_e:

$$R_e = \int_0^\infty h_e(\tau)\, d\tau \tag{9}$$

An intervention succeeds if its combined speed and coverage drive the effective reproduction number below one.

Intuitively, an intervention is most effective when it is faster than the pathogen's natural tendency to spread. This is formalized by requiring the isolation delay, $\delta_{\text{iso}}(\tau)$, to be stochastically smaller than the transmission waiting time, $t_w(\tau)$; that is, $\Delta_{\text{iso}}(\tau) \geq T_w(\tau)$ for all $\tau \geq 0$. This condition establishes a clear upper bound on the effective reproduction number under such strategies, which we denote as R_e^*:

$$\int_0^\infty h(\tau)(1 - P_{\text{iso}}\Delta_{\text{iso}}(\tau))\, d\tau = R_e \leq R_e^* = \int_0^\infty h(\tau)(1 - P_{\text{iso}}T_w(\tau))\, d\tau \tag{10}$$

We first analyze this upper bound for the ideal case of perfect coverage ($P_{\text{iso}} = 1$), where the expression simplifies to (detailed in Supplementary Material Section 2.1):

$$R_e^* = \int_0^\infty h(\tau)(1 - T_w(\tau))\, d\tau = 1 - \frac{R_0\, e^{-R_0}}{1 - e^{-R_0}} \tag{11}$$

This bound reveals two key insights. First, as $R_0 \to \infty$, the value of R_e^* approaches 1. This implies that for pathogens with very high transmissibility, the transmission waiting time defines the precise timescale for an effective intervention. The critical isolation delay, $\delta_{\text{iso}}^*(\tau)$, must therefore match this distribution:

$$\delta_{\text{iso}}^*(\tau) = t_w(\tau) = \frac{R_0\, g(\tau)\, \exp(-R_0 G(\tau))}{1 - \exp(-R_0)}. \tag{12}$$

Second, for any finite $R_0 > 1$, the value of R_e^* is strictly less than 1, which confirms that perfect isolation coverage is not necessary to achieve control.

This observation motivates finding the minimum coverage, denoted P_{iso}^*, required to bring the epidemic to its control threshold. We determine this by setting the upper bound on the reproduction number equal to one, $R_e^* = 1$, and solving for the corresponding isolation probability, P_{iso}^*. This involves solving the equation:

$$\int_0^\infty h(\tau)(1 - P_{\text{iso}}^* \Delta_{\text{iso}}^*(\tau))\, d\tau = 1, \tag{13}$$

where $\Delta_{\text{iso}}^*(\tau)$ is the CDF of the critical isolation delay, $\delta_{\text{iso}}^*(\tau)$. Solving this yields the minimum required coverage (Supplementary Materials Section 2.2):

$$P_{\text{iso}}^* = \frac{(R_0 - 1)(1 - e^{-R_0})}{R_0 - 1 + e^{-R_0}}. \tag{14}$$

Therefore, the critical intervention strategy is fully specified by two components: a requirement for the speed of intervention, $\delta_{\text{iso}}^*(\tau)$, that matches the transmission waiting time, and a minimum required coverage, P_{iso}^*. These formulas provide actionable targets for TTI interventions, linking a pathogen's intrinsic transmissibility, R_0, and generation interval, $g(\tau)$, to the necessary speed and coverage of an effective response.

Accounting for Transmission Heterogeneity

The preceding analysis relied on an assumption of homogeneous transmission, wherein each infected individual generates secondary cases according to a Poisson process with a fixed mean reproduction number, R_0 [25, 26, 27, 28]. However, the transmission dynamics of many pathogens are characterized by significant individual-level heterogeneity, or superspreading, in which a minority of infected individuals are responsible for a majority of onward transmissions. To account for this phenomenon, the framework is generalized to explicitly model such variability.

This generalization is achieved by modeling the individual transmissibility, R, not as a constant, but as a random variable drawn from a Gamma distribution with mean R_0 and dispersion parameter k:

$$f_R(R) = \frac{R^{k-1} e^{-\frac{k}{R_0} R}}{\Gamma(k)} \left(\frac{k}{R_0}\right)^k. \tag{15}$$

The number of secondary cases generated by an individual with a given transmissibility R is assumed to follow a time-varying Poisson process with hazard function $h(\tau|R) = R\, g(\tau)$. The resulting

Poisson-Gamma mixture for onward transmission yields a Negative Binomial offspring distribution for the population, which is characterized by the mean R_0 and dispersion parameter k. This model is thus capable of capturing both the average transmissibility, R_0, and the degree of transmission heterogeneity, the latter of which increases as k decreases.

A direct consequence of this heterogeneity is that the transmission waiting time is no longer uniform for the population, but is instead conditional upon an individual's specific transmissibility, R:

$$t_w(\tau|R) = \frac{R\, g(\tau)\, \exp(-R\, G(\tau))}{1 - e^{-R}}. \tag{16}$$

From a practical perspective, designing interventions tailored to individual-specific transmissibility is not feasible. We therefore aim to construct a single, population-level isolation strategy, $\delta_{\text{iso}}^{\text{het}}(\tau)$, that is effective across the entire heterogeneous population. This is achieved by averaging the conditional transmission waiting times, $t_w(\tau|R)$, over the distribution of individual transmissibility, $f_R(R)$. Such a strategy is agnostic to any single individual's infectiousness but can control the epidemic through its population-average effect, albeit with varying effectiveness at the individual level. Specifically, the average must be weighted by the probability of transmission, $(1 - e^{-R})$, and a transmissibility-related weighting function, $w(R)$. The resulting general form is:

$$\delta_{\text{iso}}^{\text{het}}(\tau) = \frac{\int_0^\infty f_R(R) w(R)(1 - e^{-R}) t_w(\tau|R)\, dR}{\int_0^\infty \int_0^\infty f_R(R) w(R)(1 - e^{-R}) t_w(\tau|R)\, d\tau dR}. \tag{17}$$

Here, $w(R)$ is a weighting function that can be chosen to prioritize certain levels of infectiousness, and the denominator normalizes the distribution.

The corresponding effective reproduction number, R_e^{het}, under an intervention with coverage P_{iso} and the general timing strategy $\delta_{\text{iso}}^{\text{het}}(\tau)$ can then be calculated. A key insight is that the effect of individual heterogeneity averages out, simplifying the expression to depend only on the population mean, R_0:

$$\begin{aligned} R_e^{\text{het}} &= \int_0^\infty \int_0^\infty f_R(R) R\, g(\tau) \left(1 - P_{\text{iso}} \Delta_{\text{iso}}^{\text{het}}(\tau)\right) dR\, d\tau \\ &= R_0 \int_0^\infty g(\tau) \left(1 - P_{\text{iso}} \Delta_{\text{iso}}^{\text{het}}(\tau)\right) d\tau, \end{aligned} \tag{18}$$

where $\Delta_{\text{iso}}^{\text{het}}(\tau) = \int_0^\tau \delta_{\text{iso}}^{\text{het}}(u) du$. We now analyze key scenarios for the weighting function $w(R)$.

Scenario 1: Unweighted Average ($w(R) = 1$)

The most straightforward approach is to use an unweighted average over the transmission waiting time, where $w(R) = 1$. In this scenario, the isolation delay is equivalent to the population-averaged transmission waiting time, $t_w^{\text{het}}(\tau)$. This integral can be solved analytically (Supplementary Materials Section 3.1), yielding:

$$\delta_{\text{iso}}^{\text{het}}(\tau)|_{w(R)=1} = t_w^{\text{het}}(\tau) = \frac{R_0 g(\tau) \left(1 + \frac{R_0}{k} G(\tau)\right)^{-(k+1)}}{1 - \left(1 + \frac{R_0}{k}\right)^{-k}}. \tag{19}$$

As shown in the Supplementary Materials Section 3.1, if we assume perfect isolation coverage ($P_{\text{iso}} = 1$), the resulting effective reproduction number can be expressed as:

$$R_e^* = \begin{cases} \dfrac{k}{k-1}\left[1 - \dfrac{R_0}{\left(1+\frac{R_0}{k}\right)^k - 1}\right], & k \neq 1, \\ (1+R_0)\left[\dfrac{1}{R_0}\ln(1+R_0) - \dfrac{1}{1+R_0}\right], & k = 1. \end{cases} \tag{20}$$

However, as detailed in the supplementary material, this isolation strategy may not guarantee outbreak control for certain values of R_0 and k, a consequence of the underlying transmission heterogeneity.

Scenario 2: Weighting by Individual Infectiousness ($w(R) = R$)

To create a more effective strategy that accounts for the fact that individuals with higher R contribute more to onward transmission, we can give more weight to their corresponding waiting times. This is achieved by setting the weighting function to be proportional to infectiousness, $w(R) = R$. The resulting isolation delay distribution can also be solved analytically (Supplementary Materials Section 3.2):

$$\delta_{\text{iso}}^{\text{het}}(\tau)|_{w(R)=R} = \frac{k(k+1)\left(\frac{k}{R_0}\right)^k g(\tau)\left(\frac{k}{R_0} + G(\tau)\right)^{-(k+2)}}{R_0\left(1 - \left(1+\frac{R_0}{k}\right)^{-(k+1)}\right)}. \tag{21}$$

This strategy is highly effective. As shown in Supplementary Materials Section 3.2, if we assume perfect isolation coverage ($P_{\text{iso}} = 1$), the resulting effective reproduction number is strictly less than 1 for all $R_0 > 1$ and $k > 0$.

$$R_e^{\text{het}}|_{w(R)=R} = \frac{1 - \Psi^{-k} - R_0\Psi^{-(k+1)}}{1 - \Psi^{-(k+1)}}, \text{ with } \Psi = 1 + R_0/k \tag{22}$$

Because control is guaranteed under perfect coverage, we can relax this requirement to find the minimum coverage, P_{iso}^* (Supplementary Materials Section 3.2), that still achieves the critical control threshold of $R_e = 1$:

$$P_{\text{iso}}^*|_{w(R)=R} = \frac{(R_0 - 1)(1 - \Psi^{-(k+1)})}{R_0 - 1 + \Psi^{-k}}. \tag{23}$$

Notably, the expressions for both the timing and coverage in this scenario depend on the dispersion parameter, k. This parameter can be more challenging to estimate from early epidemiological data compared to R_0 and $g(\tau)$, which provides a motivation to investigate control strategies that are "heterogeneity-agnostic".

Scenario 3: Homogeneous-Equivalent ($w(R) = \delta(R - R_0)$)

Recalling the insight that the population-level R_e^{het} depends only on the mean transmissibility, R_0, we therefore consider a strategy based entirely on this mean behavior. This is achieved by setting the weighting function to be the Dirac delta function, $w(R) = \delta(R - R_0)$. Due to the sifting property of the delta function, the general integral simplifies to the original transmission waiting time for a homogeneous population:

$$\delta_{\text{iso}}^{\text{het}}(\tau)|_{w(R)=\delta(R-R_0)} = \delta_{\text{iso}}^* = \frac{R_0 g(\tau) e^{-R_0 G(\tau)}}{1 - e^{-R_0}}. \tag{24}$$

Because the expression for R_e^{het} depends only on the population mean, R_0, and not the specific form of $f_R(R)$, the effectiveness of this timing strategy is independent of the underlying heterogeneity. This holds true for any distribution of individual transmissibility, not only the Gamma distribution. Therefore, the minimum isolation coverage, P_{iso}^*, required to achieve $R_e = 1$ with this strategy is also identical to the homogeneous case:

$$P_{\text{iso}}^* = \frac{(R_0 - 1)(1 - e^{-R_0})}{R_0 - 1 + e^{-R_0}}. \tag{25}$$

Notably, this robust benchmark for intervention—encompassing both the timing, δ_{iso}^*, and the required coverage, P_{iso}^*—depends only on the basic reproduction number, R_0, and the generation interval distribution, $g(\tau)$, which is "heterogeneity-agnostic". Crucially, both of these quantities are empirically measurable from data collected during the early phase of an outbreak. For instance, the generation interval $g(\tau)$ can be inferred from contact tracing data; subsequently, R_0 can be estimated from the epidemic's initial growth rate, r, via the Euler-Lotka equation:

$$R_0 = \left(\int_0^\infty e^{-r\tau} g(\tau)\, d\tau \right)^{-1}. \tag{26}$$

Assessing Pathogen' Controllability via the Transmission Waiting Time Framework

Estimating transmission waiting time for different pathogens

To evaluate the practical relevance of our theoretical framework, we apply the concepts of transmission waiting time $t_w(\tau)$ as critical isolation delay $\delta_{\text{iso}}^*(\tau)$ to a broad set of real-world pathogens, including respiratory, enteric, and hemorrhagic infections. For each pathogen, we compile key epidemiological parameters—namely, the basic reproduction number R_0 and the mean generation interval $\overline{\tau}_{\text{GI}}$—and derive the corresponding mean transmission waiting time $\overline{\tau}_{tw}$ and the isolation coverage P_{iso} required for ourbreak control (Table 1).

Table 1: Epidemiological parameters and critical control metrics for selected pathogens.

Pathogen	$\boldsymbol{R_0}$	**Mean GI (days)**	$\boldsymbol{P}_{\text{iso}}$	**Mean $t_w(\tau)$ (days)**	**Reference(s)**
Ebola	1.8	15.0	0.692	11.96	[29, 30]
Smallpox	5.0	16.0	0.992	9.24	[31, 3, 32]
Mpox	1.3	9.8	0.381	8.32	[33, 34, 35]
SARS-CoV-1	3.0	8.4	0.927	5.83	[1, 36]
Measles	15.0	11.0	1.000	4.33	[37, 38]
Plague (pneumonic)	2.4	5.0	0.854	3.71	[39, 40]
SARS-CoV-2 (Wild Type)	2.5	5.0	0.870	3.67	[41, 42]
2009 H1N1 pandemic	1.5	3.6	0.537	2.98	[43, 44]
SARS-CoV-2 (Alpha)	4.0	4.7	0.976	2.95	[45]
Influenza A (seasonal)	1.3	3.0	0.381	2.55	[46]
SARS-CoV-2 (Delta)	5.0	3.8	0.992	2.19	[47, 48]
SARS-CoV-2 (Omicron)	9.5	3.0	1.000	1.37	[47, 49, 50, 51]

This analysis reveals substantial variations in pathogen controllability. Pathogens with long generation intervals and moderate transmissibility—such as Ebola and SARS-CoV-1—offer relatively wide intervention windows, with mean transmission waiting times exceeding five days. In

contrast, highly transmissible pathogens like measles, despite having long generation intervals, require near-perfect isolation coverage within substantially shorter windows due to their explosive spread.

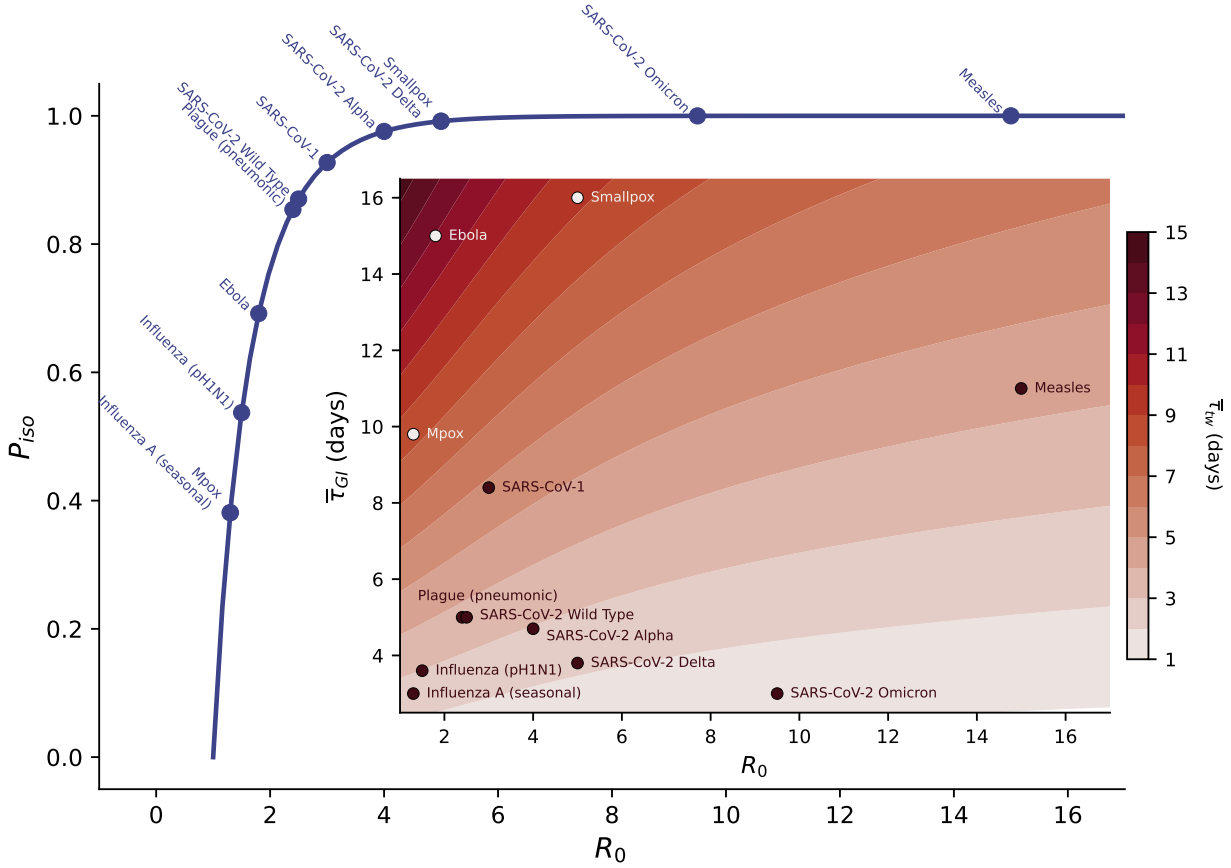

Figure 2: **Critical isolation coverage (P_{iso}) and timescale ($\overline{\tau}_{tw}$) across pathogens.** Main panel: Relationship between the basic reproduction number R_0 and the minimum isolation probability P_{iso} required for containment ($R_e = 1$). Points represent empirical pathogen estimates; the solid curve is theoretical. Inset: Heatmap illustrating the joint influence of R_0 and mean generation interval on the critical intervention timing.

At the other end of the spectrum, seasonal influenza and the 2009 H1N1 pandemic, while exhibiting low R_0 values and requiring less stringent isolation coverage, still pose challenges for containment due to their short generation intervals. This highlights that low transmissibility does not necessarily imply easier control when the pathogen spreads rapidly in-between generations.

The evolutionary trajectory of SARS-CoV-2 vividly illustrates the dynamics of its controllability over time. Early in the pandemic, the wild-type strain exhibited moderate transmissibility and manageable isolation delay requirements, enabling several countries to achieve containment through intensive test-trace-isolate strategies (detail analysis in the following sessions). However, the subsequent emergence of the Delta and Omicron variants substantially increased transmissibility while shortening generation intervals. These changes progressively tightened the requirements for both isolation coverage and intervention speed. Ultimately, the combination of high R_0 and rapid inter-generational transmission rendered local containment efforts impractical, propelling the global transition of SARS-CoV-2 toward endemic circulation.

Figure 2 reinforces these insights. The main panel illustrates the direct relationship between R_0 and the minimum isolation coverage required for containment, assuming the isolation delay follows the transmission waiting time distribution. The inset highlights how transmissibility and generation interval jointly shape the transmission waiting time distribution, which corresponds to the critical intervention timescale for pathogen controllability. Together, these visualizations underscore transmission waiting time as a central, unifying metric for evaluating the controllability of infectious disease outbreaks.

Outbreak controllability under symptom-based vs testing-based interventions: a case study of SARS-CoV-2

The extensive presymptomatic and asymptomatic transmission of SARS-CoV-2 revealed a fundamental weakness of traditional symptom-based interventions: they act too late, missing many infectious individuals and failing to interrupt transmission chains needed to bring outbreaks under control. By contrast, the widespread deployment of molecular and rapid diagnostics during the COVID-19 pandemic marked a paradigm shift—testing-based interventions detect infections independently of symptoms, enabling earlier isolation and creating opportunities to halt transmission before it begins.

In this session, using SARS-CoV-2 as a model pathogen, we apply the transmission waiting time framework to illustrate this shift. We compare isolation delays under two simplified scenarios: (1) symptom-based intervention, where individuals self-isolate upon symptom onset, and (2) testing-based intervention, where individuals isolate after receiving a positive diagnostic result. Unlike symptom-based isolation—which consistently lags behind the onset of secondary transmission—proactive testing can detect infections before the first onward transmission, opening an intervention window that symptom-based surveillance inherently misses and fundamentally altering the prospects for outbreak controllability.

Specifically, for symptom-based intervention, the isolation delay naturally follows the incubation period distribution among symptomatic infections. In Figure 3(A), we plot the distribution of SARS-CoV-2 incubation periods alongside the transmission waiting time for Wild type, Alpha, Delta, and Omicron variants. For each variant, the mean incubation period is longer than the corresponding transmission waiting time, indicating that symptom-based interventions would consistently lag behind the pace of transmission. This finding aligns with the substantial role of presymptomatic transmission observed for SARS-CoV-2. Moreover, the presence of a considerable fraction of asymptomatic infections further undermines the effectiveness of symptom-based measures against SARS-CoV-2, rendering outbreak control through this approach alone infeasible.

This pattern stands in stark contrast to SARS-CoV-1, for which the incubation period is shorter than the transmission waiting time (Figure 3(A), inset), consistent with SARS-CoV-1's minimal presymptomatic transmission [52]. Combined with SARS-CoV-1's near 100% symptomatic rate [53, 54], these features made symptom-based intervention highly effective for controlling SARS-CoV-1, as illustrated in the framework by Fraser et. al.[1].

A major technological advancement that distinguished the SARS-CoV-2 pandemic from the SARS-CoV-1 outbreak in 2003 was the widespread availability of molecular diagnostics. These include Reverse Transcription Polymerase Chain Reaction (RT-PCR) assays, which detect viral RNA, and Lateral Flow Tests (LFTs), which detect viral protein antigens using SARS-CoV-2–specific antibodies. Each diagnostic tool has distinct strengths and limitations: RT-PCR provides substantially higher sensitivity but requires centralized laboratory facilities with longer turnaround times, whereas LFTs can be performed at the point of care, delivering results within minutes but with lower sensitivity. Importantly, both methods can detect infections independent of symptom pre-

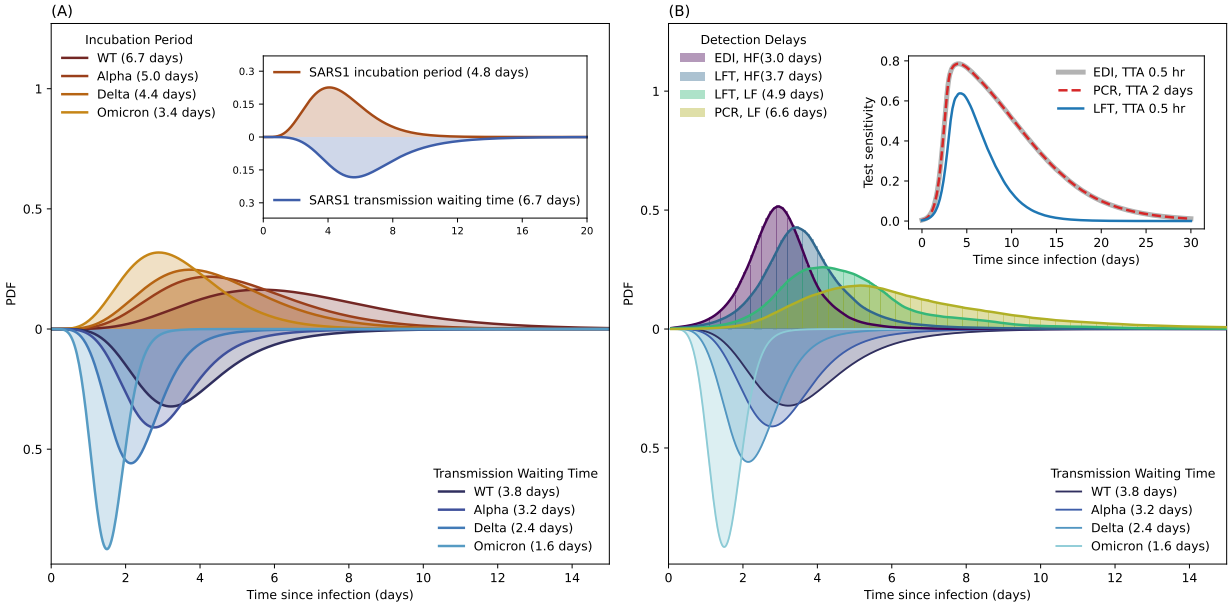

Figure 3: **Symptom-based isolation lags the transmission waiting time, while rapid testing can detect infections earlier than the transmission window of early variants.** (A) Distribution of incubation periods (symptom-based isolation delays) for SARS-CoV-2 variants (Wild type (WT), Alpha, Delta, Omicron) compared to their corresponding transmission waiting times (mean reported within parentheses). For all SARS-CoV-2 variants, the mean incubation period exceeds the transmission waiting time, implying that symptom-based isolation lags behind transmission. In contrast, for SARS1 (SARS-CoV-1), the incubation period (4.8 days) is shorter than the transmission waiting time (6.7 days), consistent with minimal presymptomatic transmission and the effectiveness of symptom-based interventions. (B) Distribution of infection detection delays under population-wide testing strategies, compared to variants corresponding transmission waiting times (mean reported within parentheses). Here we consider three types of tests: (1) conventional RT-PCR test (PCR) targeting viral RNA; (2) conventional laternal flow test (LFT) targeting viral antigen (protein); (3) emerging diagnostic innovations (EDI) that combine PCR-like sensitivity with point-of-care speed—including CRISPR-based assays, isothermal amplification platforms, and portable microfluidic PCR systems. Detection delays are shown for PCR and LFT under low frequency (LF) testing and for LFT and EDI under high frequncy (HT) testing. Transmission waiting times for Wild type (WT), Alpha, Delta, and Omicron are indicated for comparison. High-frequency testing (HF), particularly with rapid testing-turnaround (TTA) such as LFT and EDI, can reduce detection delays to levels comparable to or faster than transmission waiting times, enabling potential outbreak control for early SARS-CoV-2 variants.

sentation, enabling the identification of presymptomatic and asymptomatic cases. More recently, a wave of diagnostic innovations has emerged that combine PCR-like sensitivity with point-of-care speed—including CRISPR-based assays, isothermal amplification platforms such as LAMP and RPA, and portable microfluidic PCR systems [55, 56, 57, 58, 59, 60, 61]. Collectively, these emerging diagnostic innovations (EDI) hold promise for substantially reducing detection delays across diverse settings.

For testing-based interventions, the isolation delay is determined by the detection delay associated with a given testing scheme. Figure 3(B) shows detection delay distributions under

population-wide testing strategies compared to variant-specific transmission waiting times. Under a low-frequency (LF) scheme (testing every 3 days regardless of symptoms), both PCR (mean: 6.6 days) and LFT (mean: 4.9 days) exceeded the wild-type transmission waiting time (mean: 3.8 days). Despite higher diagnostic sensitivity, PCR produced longer delays than LFT due to its extended turnaround time (2 days vs. 0.5 hours). By contrast, high-frequency (HF) testing—particularly with rapid turnaround methods such as LFTs and EDIs—reduced detection delays to levels comparable to, or even faster than, transmission waiting times of early variants. For example, high-frequency LFT testing reduced the mean detection delay to 3.7 days, comparable to the wild-type waiting time, while EDIs further reduced delays to 3.0 days, sufficient to control early variants such as Alpha. Across all testing strategies evaluated, the proportion of infections missed remained below 10%.

Operationally, widely available and fast-turnaround testing-based intervention tools compress the isolation-delay distribution toward, and often ahead of, the transmission waiting time—the controllability threshold defined in our framework. More broadly, the transition from symptom-based to testing-based interventions redefined outbreak controllability for SARS-CoV-2, set a precedent for future pandemic response strategies, and underscored the importance of advancing and scaling these technologies to strengthen preparedness for future outbreaks.

Navigating the pathway to outbreak control: Simulation-based insights into a more realistic intervention landscape

Table 2: Summary of Incremental TTI Intervention Scenarios.

	Scenario					
TTI Operational Metric	**1**	**2**	**3**	**4**	**5**	**6**
Symptom Isolation Compliance	10%	40%	40%	40%	40%	40%
Contact Tracing Delay (days)	4	4	1	1	1	1
Testing Turnaround Time (days)	4	4	4	1	1	1
Testing Sensitivity	Low	Low	Low	Low	High	High
Population Testing Frequency (per week)	1	1	1	1	1	2

In practice, intervention methods are more complex than the simplified scenarios considered above, involving a combination of tools such as population-wide travel restrictions, contact tracing, infection screening, and symptom-based isolation. The effectiveness of these measures is shaped not only by their theoretical potential but also by operational constraints, including limited testing capacity, delays in turnaround time (TTR), incomplete contact tracing, and partial compliance with isolation. These real-world factors strongly influence the feasibility and impact of non-pharmaceutical interventions (NPIs), particularly test-trace-isolate (TTI) strategies [22, 23, 24].

To connect theoretical thresholds defined by the transmission waiting time framework with practical implementation, we conducted a simulation-based assessment using a branching process model. Each scenario is summarized by two key metrics: the mean isolation delay ($\overline{\tau}_{\text{iso}}$), representing the timeliness of intervention, and the isolation coverage (P_{iso}), representing the proportion of infections successfully isolated.

We modeled a hypothetical pathogen with a basic reproduction number of $R_0 = 6$ and a mean generation interval of 5 days, similar to SARS-CoV-2 variants. Six TTI scenarios were simulated, each incorporating incremental improvements in symptom-based isolation compliance, testing frequency and sensitivity, turnaround time, and contact tracing delay (Table 2). The result-

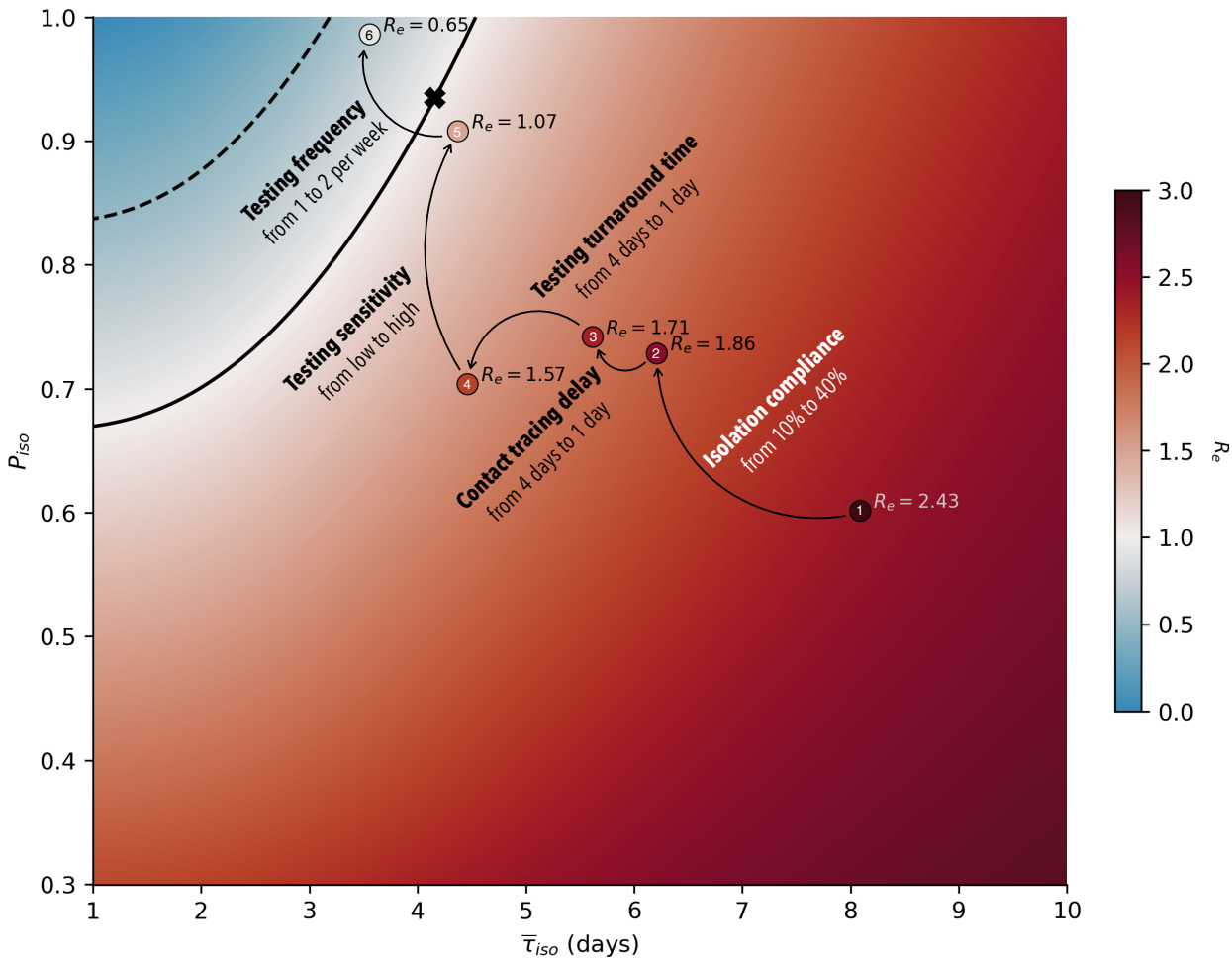

Figure 4: **Intervention landscape linking isolation timeliness $\overline{\tau}_{\text{iso}}$ and probability P_{iso} to the effective reproduction number R_e under moderate background controls**; contours show R_e=1 thresholds for R_0=3 (solid) and R_0=6 (dashed); markers denote simulated TTI scenarios; the black "X" marks the theoretical control conditions with the time-scale of intervention equals to the corresponding transmission waiting time distribution.

ing $(\overline{\tau}_{\text{iso}}, P_{\text{iso}})$ values reflect a spectrum of operational efficiency. Full model details are provided in the Supplementary Materials Section 4.

Figure 4 charts the progression of these scenarios across the intervention landscape. The heatmap displays the effective reproduction number (R_e) as a function of $\overline{\tau}_{\text{iso}}$ and P_{iso}, under a moderate background transmission setting ($R_e^{\text{lockdown}} = 3$) reflective of population-level mitigation. Contour lines denote theoretical containment thresholds ($R_e = 1$) for pathogens with moderate ($R_0 = 3$, solid line) and high ($R_0 = 6$, dashed line) transmissibility in the absence of background controls. Colored markers indicate the outcomes of the six simulated TTI scenarios. As intervention performance improves—through reductions in isolation delay and/or increases in coverage—scenarios move closer to, and in the most effective case (Scenario 6), cross the containment threshold, achieving $R_e < 1$.

These findings highlight the dual importance of speed and coverage for effective outbreak control: rapid isolation alone cannot compensate for insufficient coverage, and broad coverage is ineffective if isolation is delayed. Successful containment requires concurrent optimization of both dimensions.

This analysis provides a quantitative framework for evaluating and strengthening TTI systems under real-world constraints, offering a roadmap for tailoring containment strategies to pathogen-specific transmission dynamics.

Discussion

Despite fewer than two decades separating the SARS-CoV-1 outbreak and the SARS-CoV-2 pandemic, the landscape of outbreak interventions has changed substantially. While SARS-CoV-1 containment relied heavily on symptom-based case detection and contact tracing, the widespread pre-symptomatic and asymptomatic transmission of SARS-CoV-2 necessitated a shift toward proactive, symptom-independent strategies [6, 7, 8, 9, 10, 11]. During the early phases of attempted containment in several regions of the world, these strategies were enabled by advances such as reduced costs and increased availability of molecular diagnostics, routine population screening, and digital contact tracing—all of which allowed for earlier identification and isolation of infections beyond the reach of classical approaches [12, 62, 13, 14]. Motivated by this evolution in the intervention landscape, we developed an updated theoretical framework to evaluate pathogen controllability without relying on symptom-based surveillance.

Our work builds upon and generalizes the influential framework introduced by Fraser et al., which linked outbreak controllability to the basic reproduction number and the timing of symptom onset relative to infectiousness [1]. Fraser's framework emphasized that intervention timing and coverage were fundamentally constrained by symptom prevalence and its timing relative to infectiousness, highlighting the inherent limitations of symptom-based surveillance. In contrast, our approach directly compares the timing of interventions against the timing of transmission itself, recognizing that contemporary molecular diagnostics enable detection of pathogen spread independent of symptom onset. To quantify controllability, we introduce the concept of the transmission waiting time—the interval between acquiring infection and generating the first secondary transmission—which defines a biologically grounded, symptom-independent timescale that interventions must outpace to suppress onward spread. By modeling epidemic spread through this distribution, $t_w(\tau)$, we establish a robust upper bound on the isolation delay required for containment under both homogeneous and heterogeneous transmission assumptions. We derive closed-form expressions for the critical isolation delay distribution and the corresponding minimum required isolation coverage. These expressions depend only on two key natural history parameters—the basic reproduction number (R_0) and the generation interval distribution $g(\tau)$—both of which are measurable in the early phase of an outbreak, making our framework well-suited for real-time decision-making. Applying this approach to a diverse set of pathogens, we illustrate how intrinsic transmission characteristics constrain the feasibility of test-trace-isolate strategies for outbreak control.

The simulation analysis underscores how the timing and coverage of test-trace-isolate (TTI) strategies must align with the transmission waiting time distribution $t_w(\tau)$ to achieve containment [22, 23, 24]. While $t_w(\tau)$ defines the theoretical timing threshold that interventions must outpace, our findings highlight that practical containment hinges on achieving both sufficient speed and breadth of isolation. Incremental improvements along multiple axes—such as increasing symptom-based isolation compliance through heightened situational awareness, shortening testing and tracing delays, enhancing test sensitivity, and raising asymptomatic screening frequency—each reduce the isolation delay and/or increase isolation coverage, thereby lowering the effective reproduction number (R_e) under intervention. Importantly, $S_{\text{iso}}(\tau)$—the survival function describing infections not yet isolated—captures the joint impact of these operational factors, including tracing breadth, testing coverage, and diagnostic speed. Thus, improvements across any of these axes shift $S_{\text{iso}}(\tau)$

downward, reflecting faster or broader containment. However, no single improvement is sufficient on its own; effective containment requires coordinated implementation across these dimensions. The operational metrics identified by our framework provide pragmatic benchmarks to monitor intervention performance and guide targeted improvements. Moreover, although the current analysis focuses on TTI strategies, the same framework can accommodate other interventions—such as mask mandates, social distancing, ventilation improvements, and temporary closure of schools or venues—through their effects on contact rate and interaction structure, effectively modifying $S_{\text{iso}}(\tau)$ and the realized $t_w(\tau)$. Their multi-dimensional nature also allows tailored strategies that account for local constraints and capacities, offering a flexible and adaptive pathway toward epidemic control.

Our framework has several limitations. First, although the model explicitly incorporates heterogeneity in transmissibility, it does not account for variation in the duration or intensity of infectiousness—factors that can substantially influence the timing and effectiveness of interventions [50]. In addition, heterogeneity arises not only through variation in R_0 but also through diversity in the shape of the generation-interval distribution $g(\tau)$, as well as through contact-structure differences across settings such as households, workplaces, and community gatherings. These layers of heterogeneity may interact to shift both the mean and variance of $t_w(\tau)$, influencing achievable control in ways not captured by homogeneous models. Second, we rely on simplified mixing assumptions and do not incorporate realistic contact structures, such as heterogeneity across settings (e.g., households, workplaces, and social gatherings), variation in contact duration, or patterns of population mobility [63, 12, 62, 64]. These features are known to shape transmission dynamics and may significantly influence the impact of interventions in practice. A further limitation is that our analysis does not address the potential interplay between pathogen evolution and public health measures. The early stages of pathogen emergence in humans are often marked by rapid adaptive evolution, which can alter transmissibility, virulence, or immune escape in ways that directly affect controllability [9]. Moreover, interventions may exert selective pressures that shape evolutionary trajectories—or, conversely, limit evolution by reducing transmission opportunities. Incorporating these considerations into the controllability framework could enhance its predictive accuracy and practical utility.

In conclusion, our updated theoretical framework offers a simple yet actionable approach to evaluating pathogen controllability in the context of modern public health interventions. By anchoring control strategies to the biologically grounded concept of transmission waiting time, we derive intuitive and measurable benchmarks—namely, the critical isolation delay and the minimum required coverage—that can inform real-time decision-making. The simplicity and flexibility of this framework make it a potentially powerful tool for assessing intervention feasibility, guiding operational improvements, and supporting containment efforts in diverse epidemiological settings.

References

[1] Christophe Fraser, Steven Riley, Roy M. Anderson, and Neil M. Ferguson. Factors that make an infectious disease outbreak controllable. *Proceedings of the National Academy of Sciences*, 101(16):6146–6151, April 2004.

[2] Roy M Anderson and Robert M May. *Infectious Diseases of Humans: Dynamics and Control*. Oxford University PressOxford, May 1991.

[3] Raymond Gani and Steve Leach. Transmission potential of smallpox in contemporary populations. *Nature*, 414(6865):748–751, December 2001.

[4] Krista C. Swanson, Chiara Altare, Chea Sanford Wesseh, Tolbert Nyenswah, Tashrik Ahmed, Nir Eyal, Esther L. Hamblion, Justin Lessler, David H. Peters, and Mathias Altmann. Contact tracing performance during the Ebola epidemic in Liberia, 2014-2015. *PLOS Neglected Tropical Diseases*, 12(9):e0006762, September 2018. Publisher: Public Library of Science (PLoS).

[5] Joseph T.F. Lau, Hiyi Tsui, Mason Lau, and Xilin Yang. SARS Transmission, Risk Factors, and Prevention in Hong Kong. *Emerging Infectious Diseases*, 10(4):587–592, April 2004. Publisher: Centers for Disease Control and Prevention (CDC).

[6] Luca Ferretti, Chris Wymant, Michelle Kendall, Lele Zhao, Anel Nurtay, Lucie Abeler-Dörner, Michael Parker, David Bonsall, and Christophe Fraser. Quantifying SARS-CoV-2 transmission suggests epidemic control with digital contact tracing. *Science*, 368(6491):eabb6936, May 2020.

[7] Xi He, Eric H. Y. Lau, Peng Wu, Xilong Deng, Jian Wang, Xinxin Hao, Yiu Chung Lau, Jessica Y. Wong, Yujuan Guan, Xinghua Tan, Xiaoneng Mo, Yanqing Chen, Baolin Liao, Weilie Chen, Fengyu Hu, Qing Zhang, Mingqiu Zhong, Yanrong Wu, Lingzhai Zhao, Fuchun Zhang, Benjamin J. Cowling, Fang Li, and Gabriel M. Leung. Temporal dynamics in viral shedding and transmissibility of COVID-19. *Nature Medicine*, 26(5):672–675, May 2020. Publisher: Springer Science and Business Media LLC.

[8] Ruiyun Li, Sen Pei, Bin Chen, Yimeng Song, Tao Zhang, Wan Yang, and Jeffrey Shaman. Substantial undocumented infection facilitates the rapid dissemination of novel coronavirus (SARS-CoV-2). *Science*, 368(6490):489–493, May 2020. Publisher: American Association for the Advancement of Science (AAAS).

[9] Stephen M. Kissler, Joseph R. Fauver, Christina Mack, Scott W. Olesen, Caroline Tai, Kristin Y. Shiue, Chaney C. Kalinich, Sarah Jednak, Isabel M. Ott, Chantal B. F. Vogels, Jay Wohlgemuth, James Weisberger, John DiFiori, Deverick J. Anderson, Jimmie Mancell, David D. Ho, Nathan D. Grubaugh, and Yonatan H. Grad. Viral dynamics of acute SARS-CoV-2 infection and applications to diagnostic and public health strategies. *PLOS Biology*, 19(7):e3001333, July 2021.

[10] Daniel B. Larremore, Bryan Wilder, Evan Lester, Soraya Shehata, James M. Burke, James A. Hay, Milind Tambe, Michael J. Mina, and Roy Parker. Test sensitivity is secondary to frequency and turnaround time for COVID-19 screening. *Science Advances*, 7(1), January 2021. Publisher: American Association for the Advancement of Science (AAAS).

[11] Joel Hellewell, Sam Abbott, Amy Gimma, Nikos I Bosse, Christopher I Jarvis, Timothy W Russell, James D Munday, Adam J Kucharski, W John Edmunds, Sebastian Funk, Rosalind M

Eggo, Fiona Sun, Stefan Flasche, Billy J Quilty, Nicholas Davies, Yang Liu, Samuel Clifford, Petra Klepac, Mark Jit, Charlie Diamond, Hamish Gibbs, and Kevin Van Zandvoort. Feasibility of controlling COVID-19 outbreaks by isolation of cases and contacts. *The Lancet Global Health*, 8(4):e488–e496, April 2020. Publisher: Elsevier BV.

[12] Luca Ferretti, Chris Wymant, James Petrie, Daphne Tsallis, Michelle Kendall, Alice Ledda, Francesco Di Lauro, Adam Fowler, Andrea Di Francia, Jasmina Panovska-Griffiths, Lucie Abeler-Dörner, Marcos Charalambides, Mark Briers, and Christophe Fraser. Digital measurement of SARS-CoV-2 transmission risk from 7 million contacts. *Nature*, 626(7997):145–150, February 2024.

[13] Michael J. Mina, Roy Parker, and Daniel B. Larremore. Rethinking Covid-19 Test Sensitivity — A Strategy for Containment. *New England Journal of Medicine*, 383(22), November 2020. Publisher: Massachusetts Medical Society.

[14] Sadamori Kojaku, Laurent Hébert-Dufresne, Enys Mones, Sune Lehmann, and Yong-Yeol Ahn. The effectiveness of backward contact tracing in networks. *Nature Physics*, 17(5):652–658, May 2021. Publisher: Springer Science and Business Media LLC.

[15] Enrico Lavezzo, Elisa Franchin, Constanze Ciavarella, Gina Cuomo-Dannenburg, Luisa Barzon, Claudia Del Vecchio, Lucia Rossi, Riccardo Manganelli, Arianna Loregian, Nicolò Navarin, Davide Abate, Manuela Sciro, Stefano Merigliano, Ettore De Canale, Maria Cristina Vanuzzo, Valeria Besutti, Francesca Saluzzo, Francesco Onelia, Monia Pacenti, Saverio G. Parisi, Giovanni Carretta, Daniele Donato, Luciano Flor, Silvia Cocchio, Giulia Masi, Alessandro Sperduti, Lorenzo Cattarino, Renato Salvador, Michele Nicoletti, Federico Caldart, Gioele Castelli, Eleonora Nieddu, Beatrice Labella, Ludovico Fava, Matteo Drigo, Katy A. M. Gaythorpe, Imperial College COVID-19 Response Team, Alessandra R. Brazzale, Stefano Toppo, Marta Trevisan, Vincenzo Baldo, Christl A. Donnelly, Neil M. Ferguson, Ilaria Dorigatti, Andrea Crisanti, Imperial College COVID-19 Response Team, Kylie E. C. Ainslie, Marc Baguelin, Samir Bhatt, Adhiratha Boonyasiri, Olivia Boyd, Lorenzo Cattarino, Constanze Ciavarella, Helen L. Coupland, Zulma Cucunubá, Gina Cuomo-Dannenburg, Bimandra A. Djafaara, Christl A. Donnelly, Ilaria Dorigatti, Sabine L. Van Elsland, Rich FitzJohn, Seth Flaxman, Katy A. M. Gaythorpe, Will D. Green, Timothy Hallett, Arran Hamlet, David Haw, Natsuko Imai, Benjamin Jeffrey, Edward Knock, Daniel J. Laydon, Thomas Mellan, Swapnil Mishra, Gemma Nedjati-Gilani, Pierre Nouvellet, Lucy C. Okell, Kris V. Parag, Steven Riley, Hayley A. Thompson, H. Juliette T. Unwin, Robert Verity, Michaela A. C. Vollmer, Patrick G. T. Walker, Caroline E. Walters, Haowei Wang, Yuanrong Wang, Oliver J. Watson, Charles Whittaker, Lilith K. Whittles, Xiaoyue Xi, and Neil M. Ferguson. Suppression of a SARS-CoV-2 outbreak in the Italian municipality of Vo'. *Nature*, 584(7821):425–429, August 2020.

[16] N Ferguson, D Laydon, G Nedjati Gilani, N Imai, K Ainslie, M Baguelin, S Bhatia, A Boonyasiri, ZULMA Cucunuba Perez, G Cuomo-Dannenburg, A Dighe, I Dorigatti, H Fu, K Gaythorpe, W Green, A Hamlet, W Hinsley, L Okell, S Van Elsland, H Thompson, R Verity, E Volz, H Wang, Y Wang, P Walker, P Winskill, C Whittaker, C Donnelly, S Riley, and A Ghani. Report 9: Impact of non-pharmaceutical interventions (NPIs) to reduce COVID19 mortality and healthcare demand. Technical report, Imperial College London, March 2020.

[17] Young Joon Park, Young June Choe, Ok Park, Shin Young Park, Young-Man Kim, Jieun Kim, Sanghui Kweon, Yeonhee Woo, Jin Gwack, Seong Sun Kim, Jin Lee, Junghee Hyun, Boyeong Ryu, Yoon Suk Jang, Hwami Kim, Seung Hwan Shin, Seonju Yi, Sangeun Lee, Hee Kyoung

Kim, Hyeyoung Lee, Yeowon Jin, Eunmi Park, Seung Woo Choi, Miyoung Kim, Jeongsuk Song, Si Won Choi, Dongwook Kim, Byoung-Hak Jeon, Hyosoon Yoo, Eun Kyeong Jeong, and on behalf of the COVID-19 National Emergency Response Center, Epidemiology and Case Management Team. Contact Tracing during Coronavirus Disease Outbreak, South Korea, 2020. *Emerging Infectious Diseases*, 26(10):2465–2468, October 2020. Publisher: Centers for Disease Control and Prevention (CDC).

[18] Rachael Pung, Alex R. Cook, Calvin J. Chiew, Hannah E. Clapham, Yinxiaohe Sun, Zongbin Li, Borame L. Dickens, Stefan Ma, Kenneth Mak, Chorh Chuan Tan, Derrick Heng, Mark I-Cheng Chen, and Vernon J. Lee. Effectiveness of Containment Measures Against COVID-19 in Singapore: Implications for Other National Containment Efforts. *Epidemiology*, 32(1):79–86, January 2021. Publisher: Ovid Technologies (Wolters Kluwer Health).

[19] Giacomo Grasselli, Antonio Pesenti, and Maurizio Cecconi. Critical Care Utilization for the COVID-19 Outbreak in Lombardy, Italy: Early Experience and Forecast During an Emergency Response. *JAMA*, 323(16):1545, April 2020. Publisher: American Medical Association (AMA).

[20] Melissa M. Arons, Kelly M. Hatfield, Sujan C. Reddy, Anne Kimball, Allison James, Jesica R. Jacobs, Joanne Taylor, Kevin Spicer, Ana C. Bardossy, Lisa P. Oakley, Sukarma Tanwar, Jonathan W. Dyal, Josh Harney, Zeshan Chisty, Jeneita M. Bell, Mark Methner, Prabasaj Paul, Christina M. Carlson, Heather P. McLaughlin, Natalie Thornburg, Suxiang Tong, Azaibi Tamin, Ying Tao, Anna Uehara, Jennifer Harcourt, Shauna Clark, Claire Brostrom-Smith, Libby C. Page, Meagan Kay, James Lewis, Patty Montgomery, Nimalie D. Stone, Thomas A. Clark, Margaret A. Honein, Jeffrey S. Duchin, and John A. Jernigan. Presymptomatic SARS-CoV-2 Infections and Transmission in a Skilled Nursing Facility. *New England Journal of Medicine*, 382(22):2081–2090, May 2020. Publisher: Massachusetts Medical Society.

[21] Paavo Salminen. On the first hitting time and the last exit time for a Brownian motion to/from a moving boundary. *Advances in Applied Probability*, 20(2):411–426, June 1988. Publisher: Cambridge University Press (CUP).

[22] Billy J Quilty, Samuel Clifford, Joel Hellewell, Timothy W Russell, Adam J Kucharski, Stefan Flasche, W John Edmunds, Katherine E Atkins, Anna M Foss, Naomi R Waterlow, Kaja Abbas, Rachel Lowe, Carl A B Pearson, Sebastian Funk, Alicia Rosello, Gwenan M Knight, Nikos I Bosse, Simon R Procter, Georgia R Gore-Langton, Alicia Showering, James D Munday, Katharine Sherratt, Thibaut Jombart, Emily S Nightingale, Yang Liu, Christopher I Jarvis, Graham Medley, Oliver Brady, Hamish P Gibbs, David Simons, Jack Williams, Damien C Tully, Stefan Flasche, Sophie R Meakin, Kevin Zandvoort, Fiona Y Sun, Mark Jit, Petra Klepac, Matthew Quaife, Rosalind M Eggo, Frank G Sandmann, Akira Endo, Kiesha Prem, Sam Abbott, Rosanna Barnard, Yung-Wai D Chan, Megan Auzenbergs, Amy Gimma, C Julian Villabona-Arenas, and Nicholas G Davies. Quarantine and testing strategies in contact tracing for SARS-CoV-2: a modelling study. *The Lancet Public Health*, 6(3):e175–e183, March 2021. Publisher: Elsevier BV.

[23] Casey Middleton and Daniel B. Larremore. Modeling the transmission mitigation impact of testing for infectious diseases. *Science Advances*, 10(24):eadk5108, June 2024.

[24] Alberto Aleta, David Martín-Corral, Ana Pastore Y Piontti, Marco Ajelli, Maria Litvinova, Matteo Chinazzi, Natalie E. Dean, M. Elizabeth Halloran, Ira M. Longini Jr, Stefano Merler, Alex Pentland, Alessandro Vespignani, Esteban Moro, and Yamir Moreno. Modelling the

impact of testing, contact tracing and household quarantine on second waves of COVID-19. *Nature Human Behaviour*, 4(9):964–971, August 2020. Publisher: Springer Science and Business Media LLC.

[25] Kaiyuan Sun, Wei Wang, Lidong Gao, Yan Wang, Kaiwei Luo, Lingshuang Ren, Zhifei Zhan, Xinghui Chen, Shanlu Zhao, Yiwei Huang, Qianlai Sun, Ziyan Liu, Maria Litvinova, Alessandro Vespignani, Marco Ajelli, Cécile Viboud, and Hongjie Yu. Transmission heterogeneities, kinetics, and controllability of SARS-CoV-2. *Science*, 371(6526):eabe2424, January 2021.

[26] J. O. Lloyd-Smith, S. J. Schreiber, P. E. Kopp, and W. M. Getz. Superspreading and the effect of individual variation on disease emergence. *Nature*, 438(7066):355–359, November 2005. Publisher: Springer Science and Business Media LLC.

[27] Adam J Kucharski, Timothy W Russell, Charlie Diamond, Yang Liu, John Edmunds, Sebastian Funk, Rosalind M Eggo, Fiona Sun, Mark Jit, James D Munday, Nicholas Davies, Amy Gimma, Kevin Van Zandvoort, Hamish Gibbs, Joel Hellewell, Christopher I Jarvis, Sam Clifford, Billy J Quilty, Nikos I Bosse, Sam Abbott, Petra Klepac, and Stefan Flasche. Early dynamics of transmission and control of COVID-19: a mathematical modelling study. *The Lancet Infectious Diseases*, 20(5):553–558, May 2020. Publisher: Elsevier BV.

[28] Zhuang Shen, Fang Ning, Weigong Zhou, Xiong He, Changying Lin, Daniel P. Chin, Zonghan Zhu, and Anne Schuchat. Superspreading SARS Events, Beijing, 2003. *Emerging Infectious Diseases*, 10(2):256–260, February 2004. Publisher: Centers for Disease Control and Prevention (CDC).

[29] G. Chowell, N.W. Hengartner, C. Castillo-Chavez, P.W. Fenimore, and J.M. Hyman. The basic reproductive number of Ebola and the effects of public health measures: the cases of Congo and Uganda. *Journal of Theoretical Biology*, 229(1):119–126, July 2004.

[30] Gerardo Chowell and Hiroshi Nishiura. Transmission dynamics and control of Ebola virus disease (EVD): a review. *BMC Medicine*, 12(1):196, December 2014.

[31] Steven Riley and Neil M. Ferguson. Smallpox transmission and control: Spatial dynamics in Great Britain. *Proceedings of the National Academy of Sciences*, 103(33):12637–12642, August 2006.

[32] M. Eichner. Transmission Potential of Smallpox: Estimates Based on Detailed Data from an Outbreak. *American Journal of Epidemiology*, 158(2):110–117, July 2003.

[33] Kelly Charniga, Andrea M. McCollum, Christine M. Hughes, Benjamin Monroe, Joelle Kabamba, Robert Shongo Lushima, Toutou Likafi, Beatrice Nguete, Elisabeth Pukuta, Elisabeth Muyamuna, Jean-Jacques Muyembe Tamfum, Stomy Karhemere, Didine Kaba, and Yoshinori Nakazawa. Updating Reproduction Number Estimates for Mpox in the Democratic Republic of Congo Using Surveillance Data. *The American Journal of Tropical Medicine and Hygiene*, 110(3):561–568, March 2024.

[34] Antoine Gessain, Emmanuel Nakoune, and Yazdan Yazdanpanah. Monkeypox. *New England Journal of Medicine*, 387(19):1783–1793, November 2022.

[35] Zachary J. Madewell, Kelly Charniga, Nina B. Masters, Jason Asher, Lily Fahrenwald, William Still, Judy Chen, Naama Kipperman, David Bui, Meghan Shea, Katharine Saunders, Lori Saathoff-Huber, Shannon Johnson, Khalil Harbi, Abby L. Berns, Taidy Perez, Emily Gateley,

Ian H. Spicknall, Yoshinori Nakazawa, Thomas L. Gift, and 2022 Mpox Outbreak Response Team2. Serial Interval and Incubation Period Estimates of Monkeypox Virus Infection in 12 Jurisdictions, United States, May–August 2022. *Emerging Infectious Diseases*, 29(4):818–821, April 2023.

[36] Marc Lipsitch, Ted Cohen, Ben Cooper, James M. Robins, Stefan Ma, Lyn James, Gowri Gopalakrishna, Suok Kai Chew, Chorh Chuan Tan, Matthew H. Samore, David Fisman, and Megan Murray. Transmission Dynamics and Control of Severe Acute Respiratory Syndrome. *Science*, 300(5627):1966–1970, June 2003.

[37] Paul E M Fine and Jacqueline A Clarkson. Measles in England and Wales—II: The Impact of the Measles Vaccination Programme on the Distribution of Immunity in the Population. *International Journal of Epidemiology*, 11(1):15–25, 1982.

[38] Bryan T. Grenfell, Ottar N. Bjørnstad, and Bärbel F. Finkenstädt. DYNAMICS OF MEASLES EPIDEMICS: SCALING NOISE, DETERMINISM, AND PREDICTABILITY WITH THE TSIR MODEL. *Ecological Monographs*, 72(2):185–202, May 2002. Publisher: Wiley.

[39] H. Nishiura. Transmission potential of primary pneumonic plague: time inhomogeneous evaluation based on historical documents of the transmission network. *Journal of Epidemiology & Community Health*, 60(7):640–645, July 2006.

[40] Maimuna S. Majumder, Emily L. Cohn, Mauricio Santillana, and John S. Brownstein. Estimation of Pneumonic Plague Transmission in Madagascar, August–November 2017. *PLoS Currents*, 2018.

[41] Qun Li, Xuhua Guan, Peng Wu, Xiaoye Wang, Lei Zhou, Yeqing Tong, Ruiqi Ren, Kathy S.M. Leung, Eric H.Y. Lau, Jessica Y. Wong, Xuesen Xing, Nijuan Xiang, Yang Wu, Chao Li, Qi Chen, Dan Li, Tian Liu, Jing Zhao, Man Liu, Wenxiao Tu, Chuding Chen, Lianmei Jin, Rui Yang, Qi Wang, Suhua Zhou, Rui Wang, Hui Liu, Yinbo Luo, Yuan Liu, Ge Shao, Huan Li, Zhongfa Tao, Yang Yang, Zhiqiang Deng, Boxi Liu, Zhitao Ma, Yanping Zhang, Guoqing Shi, Tommy T.Y. Lam, Joseph T. Wu, George F. Gao, Benjamin J. Cowling, Bo Yang, Gabriel M. Leung, and Zijian Feng. Early Transmission Dynamics in Wuhan, China, of Novel Coronavirus–Infected Pneumonia. *New England Journal of Medicine*, 382(13):1199–1207, March 2020. Publisher: Massachusetts Medical Society.

[42] Zunyou Wu and Jennifer M. McGoogan. Characteristics of and Important Lessons From the Coronavirus Disease 2019 (COVID-19) Outbreak in China: Summary of a Report of 72314 Cases From the Chinese Center for Disease Control and Prevention. *JAMA*, 323(13):1239, April 2020. Publisher: American Medical Association (AMA).

[43] Laura Forsberg White, Jacco Wallinga, Lyn Finelli, Carrie Reed, Steven Riley, Marc Lipsitch, and Marcello Pagano. Estimation of the reproductive number and the serial interval in early phase of the 2009 influenza A/H1N1 pandemic in the USA. *Influenza and Other Respiratory Viruses*, 3(6):267–276, November 2009.

[44] Christophe Fraser, Christl A. Donnelly, Simon Cauchemez, William P. Hanage, Maria D. Van Kerkhove, T. Déirdre Hollingsworth, Jamie Griffin, Rebecca F. Baggaley, Helen E. Jenkins, Emily J. Lyons, Thibaut Jombart, Wes R. Hinsley, Nicholas C. Grassly, Francois Balloux, Azra C. Ghani, Neil M. Ferguson, Andrew Rambaut, Oliver G. Pybus, Hugo Lopez-Gatell,

Celia M. Alpuche-Aranda, Ietza Bojorquez Chapela, Ethel Palacios Zavala, Dulce Ma. Espejo Guevara, Francesco Checchi, Erika Garcia, Stephane Hugonnet, Cathy Roth, and The WHO Rapid Pandemic Assessment Collaboration. Pandemic Potential of a Strain of Influenza A (H1N1): Early Findings. *Science*, 324(5934):1557–1561, June 2009.

[45] Nicholas G. Davies, Sam Abbott, Rosanna C. Barnard, Christopher I. Jarvis, Adam J. Kucharski, James D. Munday, Carl A. B. Pearson, Timothy W. Russell, Damien C. Tully, Alex D. Washburne, Tom Wenseleers, Amy Gimma, William Waites, Kerry L. M. Wong, Kevin Van Zandvoort, Justin D. Silverman, CMMID COVID-19 Working Group, COVID-19 Genomics UK (COG-UK) Consortium, Karla Diaz-Ordaz, Ruth Keogh, Rosalind M. Eggo, Sebastian Funk, Mark Jit, Katherine E. Atkins, and W. John Edmunds. Estimated transmissibility and impact of SARS-CoV-2 lineage B.1.1.7 in England. *Science*, 372(6538):eabg3055, April 2021.

[46] Matthew Biggerstaff, Simon Cauchemez, Carrie Reed, Manoj Gambhir, and Lyn Finelli. Estimates of the reproduction number for seasonal, pandemic, and zoonotic influenza: a systematic review of the literature. *BMC Infectious Diseases*, 14(1):480, December 2014.

[47] Zachary J. Madewell, Yang Yang, Ira M. Longini, M. Elizabeth Halloran, Alessandro Vespignani, and Natalie E. Dean. Rapid review and meta-analysis of serial intervals for SARS-CoV-2 Delta and Omicron variants. *BMC Infectious Diseases*, 23(1):429, June 2023.

[48] Ying Liu and Joacim Rocklöv. The reproductive number of the Delta variant of SARS-CoV-2 is far higher compared to the ancestral SARS-CoV-2 virus. *Journal of Travel Medicine*, 28(7):taab124, October 2021.

[49] Ying Liu and Joacim Rocklöv. The effective reproductive number of the Omicron variant of SARS-CoV-2 is several times relative to Delta. *Journal of Travel Medicine*, 29(3):taac037, May 2022.

[50] Kaiyuan Sun, Stefano Tempia, Jackie Kleynhans, Anne Von Gottberg, Meredith L. McMorrow, Nicole Wolter, Jinal N. Bhiman, Jocelyn Moyes, Mignon Du Plessis, Maimuna Carrim, Amelia Buys, Neil A. Martinson, Kathleen Kahn, Stephen Tollman, Limakatso Lebina, Floidy Wafawanaka, Jacques D. Du Toit, Francesc Xavier Gómez-Olivé, Thulisa Mkhencele, Cécile Viboud, and Cheryl Cohen. SARS-CoV-2 transmission, persistence of immunity, and estimates of Omicron's impact in South African population cohorts. *Science Translational Medicine*, 14(659):eabo7081, August 2022.

[51] Juliet R. C. Pulliam, Cari Van Schalkwyk, Nevashan Govender, Anne Von Gottberg, Cheryl Cohen, Michelle J. Groome, Jonathan Dushoff, Koleka Mlisana, and Harry Moultrie. Increased risk of SARS-CoV-2 reinfection associated with emergence of Omicron in South Africa. *Science*, 376(6593), May 2022. Publisher: American Association for the Advancement of Science (AAAS).

[52] Christl A Donnelly, Azra C Ghani, Gabriel M Leung, Anthony J Hedley, Christophe Fraser, Steven Riley, Laith J Abu-Raddad, Lai-Ming Ho, Thuan-Quoc Thach, Patsy Chau, King-Pan Chan, Tai-Hing Lam, Lai-Yin Tse, Thomas Tsang, Shao-Haei Liu, James H B Kong, Edith M C Lau, Neil M Ferguson, and Roy M Anderson. Epidemiological determinants of spread of causal agent of severe acute respiratory syndrome in hong kong. 361:1761–1766.

[53] Nelson Lee, David Hui, Alan Wu, Paul Chan, Peter Cameron, Gavin M Joynt, Anil Ahuja, Man Yee Yung, C B Leung, K F To, S F Lui, C C Szeto, Sydney Chung, and Joseph J Y Sung. A major outbreak of severe acute respiratory syndrome in hong kong. 348:1986–1994.

[54] Thomas G Ksiazek, Dean Erdman, Cynthia S Goldsmith, Sherif R Zaki, Teresa Peret, Shannon Emery, Suxiang Tong, Carlo Urbani, James A Comer, Wilina Lim, Pierre E Rollin, Scott F Dowell, Ai-Ee Ling, Charles D Humphrey, Wun-Ju Shieh, Jeannette Guarner, Christopher D Paddock, Paul Rota, Barry Fields, Joseph DeRisi, Jyh-Yuan Yang, Nancy Cox, James M Hughes, James W LeDuc, William J Bellini, Larry J Anderson, and SARS Working Group. A novel coronavirus associated with severe acute respiratory syndrome. 348:1953–1966.

[55] Jonathan S Gootenberg, Omar O Abudayyeh, Jeong Wook Lee, Patrick Essletzbichler, Aaron J Dy, Julia Joung, Vanessa Verdine, Nina Donghia, Nichole M Daringer, Catherine A Freije, et al. Nucleic acid detection with crispr-cas13a/c2c2. *Science*, 356(6336):438–442, 2017.

[56] Nicole L Welch, Meilin Zhu, Catherine Hua, Juliane Weller, Marzieh Ezzaty Mirhashemi, Tien G Nguyen, Sreekar Mantena, Matthew R Bauer, Bennett M Shaw, Cheri M Ackerman, et al. Multiplexed crispr-based microfluidic platform for clinical testing of respiratory viruses and identification of sars-cov-2 variants. *Nature medicine*, 28(5):1083–1094, 2022.

[57] Jon Arizti-Sanz, A'Doriann Bradley, Yibin B Zhang, Chloe K Boehm, Catherine A Freije, Michelle E Grunberg, Tinna-Solveig F Kosoko-Thoroddsen, Nicole L Welch, Priya P Pillai, Sreekar Mantena, et al. Simplified cas13-based assays for the fast identification of sars-cov-2 and its variants. *Nature biomedical engineering*, 6(8):932–943, 2022.

[58] Viet Loan Dao Thi, Konrad Herbst, Kathleen Boerner, Matthias Meurer, Lukas PM Kremer, Daniel Kirrmaier, Andrew Freistaedter, Dimitrios Papagiannidis, Carla Galmozzi, Megan L Stanifer, et al. A colorimetric rt-lamp assay and lamp-sequencing for detecting sars-cov-2 rna in clinical samples. *Science translational medicine*, 12(556):eabc7075, 2020.

[59] Yangyang Sun, Lei Yu, Chengxi Liu, Shanting Ye, Wei Chen, Dechang Li, and Weiren Huang. One-tube sars-cov-2 detection platform based on rt-rpa and crispr/cas12a. *Journal of translational medicine*, 19(1):74, 2021.

[60] Leon Peto, Gillian Rodger, Daniel P Carter, Karen L Osman, Mehmet Yavuz, Katie Johnson, Mohammad Raza, Matthew D Parker, Matthew D Wyles, Monique Andersson, et al. Diagnosis of sars-cov-2 infection with lampore, a high-throughput platform combining loop-mediated isothermal amplification and nanopore sequencing. *Journal of clinical microbiology*, 59(6):10–1128, 2021.

[61] Anurup Ganguli, Ariana Mostafa, Jacob Berger, Mehmet Y Aydin, Fu Sun, Sarah A Stewart de Ramirez, Enrique Valera, Brian T Cunningham, William P King, and Rashid Bashir. Rapid isothermal amplification and portable detection system for sars-cov-2. *Proceedings of the National Academy of Sciences*, 117(37):22727–22735, 2020.

[62] Michelle Kendall, Luca Ferretti, Chris Wymant, Daphne Tsallis, James Petrie, Andrea Di Francia, Francesco Di Lauro, Lucie Abeler-Dörner, Harrison Manley, Jasmina Panovska-Griffiths, Alice Ledda, Xavier Didelot, and Christophe Fraser. Drivers of epidemic dynamics in real time from daily digital COVID-19 measurements. *Science*, 385(6710), August 2024. Publisher: American Association for the Advancement of Science (AAAS).

[63] Christophe Fraser. Estimating Individual and Household Reproduction Numbers in an Emerging Epidemic. *PLoS ONE*, 2(8):e758, August 2007.

[64] Juanjuan Zhang, Maria Litvinova, Yuxia Liang, Yan Wang, Wei Wang, Shanlu Zhao, Qianhui Wu, Stefano Merler, Cécile Viboud, Alessandro Vespignani, Marco Ajelli, and Hongjie Yu. Changes in contact patterns shape the dynamics of the COVID-19 outbreak in China. *Science*, 368(6498):1481–1486, June 2020. Publisher: American Association for the Advancement of Science (AAAS).

Conflict of interest statement

P.C.S. is a co-founder of, shareholder in, and consultant to Sherlock Biosciences, Inc. and Delve Bio. CF has received subcontracts from Johns Hopkins University to the University of Oxford to support ongoing research with the Rakai Community Cohort Studies, including the projects Longview and Hard to Reach. CF has received a contract from UKHSA for research related to the NHS COVID-19 app. CF has received research funding for the PANGAEA-HIV consortium for modelling and molecular epidemiology of HIV-1 1in Eastern and Southern Africa.

Funding statement

C.Y.S. was funded by the Harvard Global Health Institute Research & Internships Grant (192206).